

# Na<sup>+</sup> channel inactivation: a comparative study between pancreatic islet $\beta$ -cells and adrenal chromaffin cells in rat

Xue-Lin Lou\*†, Xiao Yu\*, Xiao-Ke Chen\*, Kai-Lai Duan\*, Li-Ming He†, An-Lian Qu†, Tao Xu† and Zhuan Zhou\*†

\*Institute of Neuroscience, Shanghai Institutes for Biological Sciences, Chinese Academy of Sciences, Shanghai 200031, China and †Institute of Biophysics and Biochemistry, Huazhong University of Science and Technology, Wuhan 430074, China

A comparative study was carried out on the inactivation of Na<sup>+</sup> channels in two types of endocrine cells in rats,  $\beta$ -cells and adrenal chromaffin cells (ACCs), using patch-clamp techniques. The  $\beta$ -cells were very sensitive to hyperpolarization; the Na<sup>+</sup> currents increased ninefold when the holding potential was shifted from  $-70$  mV to  $-120$  mV. ACCs were not sensitive to hyperpolarization. The half-inactivation voltages were  $-90$  mV (rat  $\beta$ -cells) and  $-62$  mV (ACCs). The time constant for recovery from inactivation at  $-70$  mV was 10.5 times slower in  $\beta$ -cells (60 ms) than in ACCs (5.7 ms). The rate of Na<sup>+</sup>-channel inactivation at physiological resting potential was more than three times slower in  $\beta$ -cells than in ACCs. Na<sup>+</sup> influx through Na<sup>+</sup> channels had no effect on the secretory machinery in rat  $\beta$ -cells. However, these 'silent Na<sup>+</sup> channels' could contribute to the generation of action potentials in some conditions, such as when the cell is hyperpolarized. It is concluded that the fractional availability of Na<sup>+</sup> channels in  $\beta$ -cells at a holding potential of  $-70$  mV is about 15 % of that in ACCs. This value in rat  $\beta$ -cells is larger than that observed in mouse (0 %), but is smaller than those observed in human or dog (90 %).

(Resubmitted 13 October 2002; accepted after revision 13 January 2003; first published online 7 February 2003)

**Corresponding author** Z. Zhou: Institute of Neuroscience, 320 Yue-Yang Road, Shanghai 200031, China.  
Email: zzhou@ion.ac.cn

The voltage-gated Na<sup>+</sup> channel is one of the two principal elements of an action potential in most excitable cells, including neurons, muscles and endocrine cells (Hille, 1992). The pancreatic islet  $\beta$ -cell is a type of excitable endocrine cell that secretes insulin (Henquin *et al.* 1987). Functional failure in  $\beta$ -cells may cause diabetes (Ashcroft & Rorsman, 1990). While much is known about the functions and biophysics of Ca<sup>2+</sup> channels and K<sup>+</sup> channels in  $\beta$ -cells (Ashcroft *et al.* 1984; Rorsman & Trube, 1986; Ashcroft & Rorsman, 1990; Satin *et al.* 1994), relatively little is known about the Na<sup>+</sup> channels in  $\beta$ -cells (Plant, 1988; Pressel & Mislner, 1990).

Inactivation is a major and distinct property of voltage-gated Na<sup>+</sup> channels. Fast action potentials in excitable cells have a fast rising phase and a fast decay phase. Theoretically and experimentally, one molecular mechanism of open-channel inactivation has been explained by the 'chain and ball' theory (Armstrong & Bezanilla, 1977; Aldrich, 2001; Zhou *et al.* 2001). In K<sup>+</sup> channels, an open channel can be blocked by a charged ball (part of the channel protein), which is electrically attracted by a charge inside the channel (Zhou *et al.* 2001). It is possible that Na<sup>+</sup>-channel inactivation shares a similar mechanism. A closed channel may also be inactivated. Thus, Na<sup>+</sup> channels in some

$\beta$ -cells are inactivated at the resting potential ( $-70$  mV), which does not reach the activation potential (minimum  $-50$  mV; Hiriart & Matteson, 1988; Plant, 1988).

There is considerable diversity in the properties of Na<sup>+</sup> channels among different species. For example, in mouse  $\beta$ -cells Na<sup>+</sup> channels inactivate completely at the resting potential and TTX cannot block action potentials (Plant, 1988). In dog and human  $\beta$ -cells, however, action potentials are TTX sensitive (Barnett *et al.* 1995; Pressel & Mislner, 1991). In rat  $\beta$ -cells, some preliminary reports suggest that Na<sup>+</sup> channels also show considerable inactivation at the resting potential (Pace, 1979; Hiriart & Matteson, 1988).

Adrenal chromaffin cells (ACCs) and neurons share similar action potentials and voltage-gated channels, including Na<sup>+</sup> channels (Artalejo, 1995). Thus, many patch-clamp studies on voltage-gated Ca<sup>2+</sup> and K<sup>+</sup> channels have used ACCs as model neurons (Fenwick *et al.* 1982b; Artalejo *et al.* 1992; Neely & Lingle, 1992). It is known that in rat, the action potentials in pancreatic  $\beta$ -cells and ACCs are very different (Pace, 1979; Kidokoro & Ritchie, 1980). Step-stimulus-induced action potentials in ACCs have high amplitudes (typically 50 mV) and many cells fire burst-type spikes (Zhou & Mislner, 1995). In contrast, the same step stimulus in rat  $\beta$ -cells induces only single action

potentials followed by a plateau (Zhou & Misler, 1996). In the present study, we investigated in parallel the biophysical properties of Na<sup>+</sup>-channel inactivation in rat  $\beta$ -cells and ACCs. In some cases, mouse  $\beta$ -cells were also tested. The two aims were: (1) to compare the Na<sup>+</sup>-channel inactivation in  $\beta$ -cells and ACCs in rat and (2) to evaluate the physiological role of Na<sup>+</sup> channels in rat  $\beta$ -cells. We found that the level of steady-state inactivation in rat  $\beta$ -cells lies between those of mouse  $\beta$ -cells and rat ACCs. Thus, Na<sup>+</sup> channels in rat  $\beta$ -cells may play a role that is intermediate between that of mouse  $\beta$ -cells and ACCs.

## METHODS

### Cells and solutions

Pancreatic islet  $\beta$ -cells of adult Wistar rats (150–250 g) were isolated and cultured as described previously (Ashcroft *et al.* 1984; Zhou & Misler, 1996). Briefly, rats were killed by cervical dislocation and the islets were collected from the pancreas by collagenase digestion (3.3 mg ml<sup>-1</sup> collagenase V for 30 min). Single  $\beta$ -cells were isolated from islets treated with Dispase-II (0.3 mg ml<sup>-1</sup> for 12 min) and cultured in a standard CO<sub>2</sub> incubator for up to 1 week.  $\beta$ -Cells were identified by their relatively large size and their functional properties, such as their response to glucose and the presence of K(ATP) channels (Fig. 1).

ACCs of adult Wistar rats (250–300 g), killed with an overdose of ether, were isolated and cultured as described previously (Zhou & Misler, 1995; Wu *et al.* 2002). Briefly, single cells were obtained after 40 min digestion in the enzyme solution. The cells were cultured with Dulbecco's modified Eagle's medium (DMEM) in a CO<sub>2</sub> incubator. Cells of 2–6 days' culture were used in experiments. The use and care of animals followed the guidelines of the Shanghai Institutes of Biological Sciences Animal Research Advisory Committee.

DMEM for cell culture contained 17.72 mM H<sup>+</sup>-Hepes, 7.28 mM Na<sup>+</sup>-Hepes, 44 mM NaHCO<sub>3</sub>, 10 mg ml<sup>-1</sup> DMEM, 100 IU ml<sup>-1</sup> penicillin G, 100 ug ml<sup>-1</sup> streptomycin, 0.6% vitamin C and 10% fetal bovine serum. The standard bath solution for  $\beta$ -cells contained (mM): 138 NaCl, 5.6 KCl, 1.2 MgCl<sub>2</sub>, 2.6 CaCl<sub>2</sub>, 3 glucose, 5 Hepes (pH 7.4). For ACCs, the standard bath solution contained (mM): 145 NaCl, 2.8 KCl, 1 MgCl<sub>2</sub>, 2 CaCl<sub>2</sub>, 10 glucose, 10 Hepes (pH 7.4). To record Na<sup>+</sup> currents, the external solution was modified by adding 0.5 mM CdCl<sub>2</sub> and replacing 20 mM NaCl with 20 mM TEA-Cl. The standard internal solution contained (mM): 125 CsCl, 10 NaCl, 1.0 MgCl<sub>2</sub>, 3 MgATP, 5 Hepes. In cell-attached recordings, the pipette solution contained (mM): 63.7 KCl, 28.35 K<sub>2</sub>SO<sub>4</sub>, 11.8 NaCl, 1.0 MgCl<sub>2</sub>, 47.2 sucrose, 20 Hepes (pH 7.2). DMEM, Dispase-II, fetal bovine serum and BSA were from Gibco; Fura-2 AM was from Molecular Probes, and all other chemicals were obtained from Sigma.

### Patch-clamp recording from single cells

Patch pipettes pulled from borosilicate glass capillaries had resistances of 2–6 M $\Omega$  when filled with internal solution. To reduce errors from the access resistance ( $R_s$ ), cells were included only when the  $R_s$  of the perforated patch was smaller than 10 M $\Omega$  (ACCs) or 20 M $\Omega$  ( $\beta$ -cells). In addition,  $R_s$  compensation was > 80%. Membrane currents and action potentials were recorded with an EPC-9 patch-clamp amplifier and PULSE software (HEKA Electronic, Germany). The membrane capacitance ( $C_m$ ) measurements were carried out by the built-in lock-in amplifier of

the EPC-9 (Horn & Marty, 1988; Lindau & Neher, 1988; Falke *et al.* 1989; Zhang & Zhou, 2002). The data sample rate was 2.5 kHz for single-channel recording and 5–20 kHz for whole-cell recordings. The data were low-pass filtered at 300 Hz for single-channel recordings and 2.5 kHz for whole-cell recordings.

During recording, drugs and control/wash solutions were puffed locally onto the cell via an RCP-2B multichannel microperfusion system (INBIO, Wuhan, China), which allowed fast (< 100 ms) electronic change of local solutions between seven solution channels. The tip (100  $\mu$ m diameter) of the puffer pipette was located about 120  $\mu$ m from the cell. As determined by the conductance tests, the solution around a cell under study was fully controlled by the application solution, provided the application flow speed was 100  $\mu$ l min<sup>-1</sup> or greater. All pharmacological experiments met this criterion (Wu *et al.* 2002).

Intracellular Ca<sup>2+</sup> was measured by Fura-2 fluorescence assay, as described previously (Zhou & Neher, 1993). The cells were incubated in 5  $\mu$ M Fura-2 AM for 20 min at room temperature. All experiments were carried out at room temperature (22–24 °C), except for the  $\beta$ -cell  $C_m$  measurements shown in Fig. 8, where cells were bathed at 31–33 °C.

### Data analysis

Data was analysed with IGOR Pro3.12 software (Wavemetrics, Lake Oswego, OR, USA). Unless stated otherwise, the data are presented as means  $\pm$  S.E.M., significance was tested by Student's *t* test, and a difference was considered significant if  $P < 0.05$ . The h-infinity curves (Fig. 3) were fitted with the Boltzmann function:

$$I/I_{\max} = (1 - \exp(-V + V_{50})/k) - 1,$$

where  $I$  is the current,  $I_{\max}$  is the maximum current,  $V_{50}$  is the voltage of half steady-state inactivation, and  $k$  is the slope factor (mV<sup>-1</sup>), which is related to the voltage dependence of the inactivation process.

## RESULTS

### Basic functional characteristics of rat $\beta$ -cells

$\beta$ -Cells can be identified according to their responses to glucose added to the bath solution (Ashcroft *et al.* 1984; Rorsman & Trube, 1986; Plant, 1988; Pressel & Misler, 1990). Alternatively, the presence of K(ATP) channels, characterized by bursting of 2–4 pA single-channel currents in the on-cell configuration, is also used as a mark of  $\beta$ -cells in bathing solutions containing low concentrations of glucose. After exposing cells to high concentrations of glucose, biphasic currents ('action currents') are often observed in the on-cell configuration.

In standard external and internal solutions (Fig. 1A, top and bottom traces), the typical burst K(ATP) channel currents were recorded when the pipette potential was held at 0 mV. The conductance of the single channel currents was 48 pS, which is consistent with previous reports (Ashcroft *et al.* 1984; Misler *et al.* 1986). Tolbutamide (500  $\mu$ M) blocked the K(ATP) currents and induced the biphasic action currents (Fig. 1A, middle trace), which might be generated by action potentials in the cells (Fenwick *et al.* 1982a). Another 'signature' of  $\beta$ -cells is their response to glucose. As shown in Fig. 1B, 10 mM glucose induced a [Ca<sup>2+</sup>]<sub>i</sub> increase in a single

cell, indicating that this was a  $\beta$ -cell (Zeng *et al.* 1999). The criteria illustrated in Fig. 1 were used regularly, and we found that more than 90 % of cells tested were  $\beta$ -cells.

### Hyperpolarization increased Na<sup>+</sup> currents in $\beta$ -cells but not in ACCs

In 90 % of rat  $\beta$ -cells, there were only small, voltage-gated, fast-inactivation currents when the holding and test potentials were  $-70$  mV and  $+10$  mV, respectively. However, in the same cells, the fast-inactivation currents were dramatically increased (by about ninefold) when the holding potential was reduced to  $-120$  mV (Fig. 2). Since mouse  $\beta$ -cells have been studied intensively in many laboratories, we also included data from mouse  $\beta$ -cells for comparison. Consistent with the literature, the fast inward current was completely absent in mouse  $\beta$ -cells when the holding potential was  $-70$  mV. These fast inward currents were sensitive to TTX (see Fig. 7A), indicating that the channels involved were voltage-gated Na<sup>+</sup> channels. Similar observations have been reported in mouse (Plant, 1988), but not in cells from humans or dogs (Pressel & Mislner, 1991; Barnett *et al.* 1995). In the typical case of Fig. 2A (rat  $\beta$ -cells), the Na<sup>+</sup> current increased 10-fold (from  $-108$  to  $-1090$  pA) when the holding potential was changed from  $-70$  mV to  $-120$  mV. In contrast, there was no change in Na<sup>+</sup> current

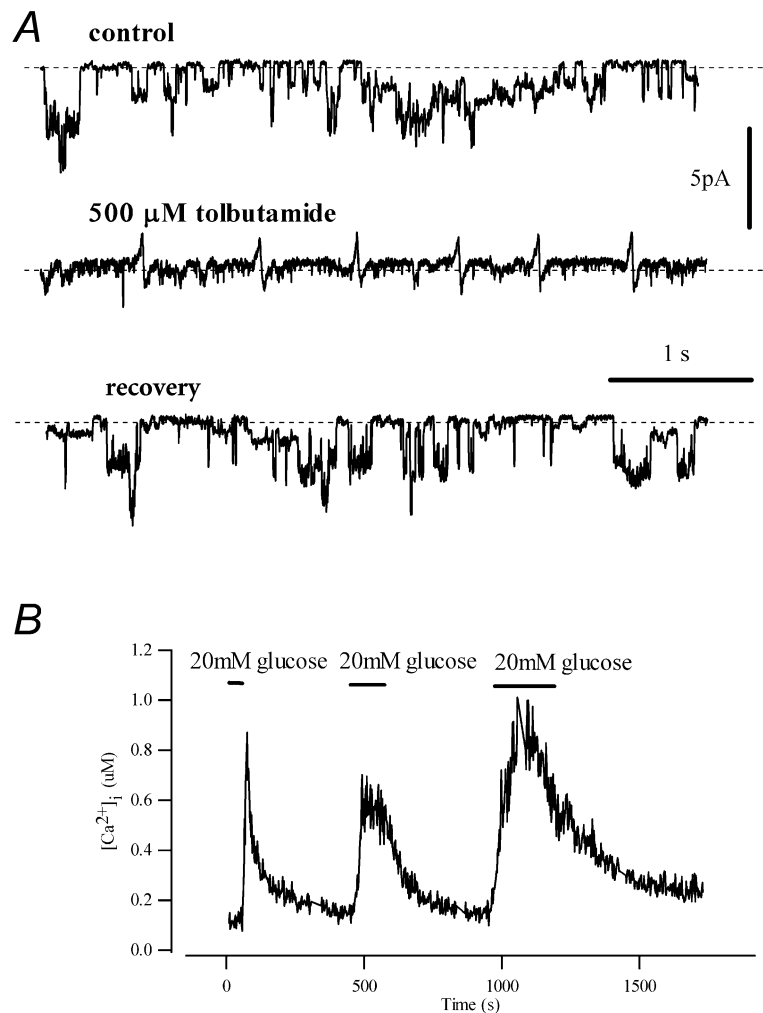
(3.2 nA) when the same change of holding potential was made in ACCs (Fig. 2A, right panels). This drastic difference in Na<sup>+</sup>-channel sensitivity to hyperpolarization between the two types of endocrine cells might have significant consequences for cell excitation, because the physiological resting potentials ( $-50$  to  $-80$  mV) are similar for both cell types (Ashcroft & Rorsman, 1990; Zhou & Mislner, 1995). Figure 2B and C shows that the differences in inactivation between the three cell types are statistically significant.

### Steady-state inactivation

The curves for steady-state inactivation were very different between the two cell types (Fig. 3). The holding potential ranges were  $-150$  to  $-40$  mV for rat and mouse  $\beta$ -cells, and  $-150$  mV to  $+10$  mV for ACCs. In  $\beta$ -cells, the holding potential for half-inactivation of the Na<sup>+</sup> current,  $E_{50}$ , was  $-90$  mV for rat and  $-110$  mV for mouse. At the normal resting potential of  $-70$  mV, only 15 % of Na<sup>+</sup> channels could be activated by depolarization in rat  $\beta$ -cells. No Na<sup>+</sup> currents could be activated from a resting potential of  $-70$  mV in mouse  $\beta$ -cells. In ACCs, however, the  $E_{50}$  was  $-62$  mV. At  $-70$  mV, 70 % of Na<sup>+</sup> channels could be activated by depolarization. The slope factors were  $-7.6$  mV and  $-9.7$  mV for rat and mouse  $\beta$ -cells, respectively, and  $-9.1$  mV for ACCs.

### Figure 1. Identification of pancreatic islet $\beta$ -cells

**A**, tolbutamide blocked single channel activity of K(ATP) reversibly. Top trace, typical burst of single K(ATP) channel currents in cell-attached configuration with high-K<sup>+</sup> pipette solution and standard bath solution. Middle trace, 500  $\mu$ M tolbutamide blocked K(ATP) current and elicited the typical biphasic spikes of 'action currents'. Bottom trace, recovery of K(ATP) activity after washout of tolbutamide ( $n = 40$ ). **B**, 20 mM glucose evoked increases in [Ca<sup>2+</sup>]<sub>i</sub> from basal level (110 nM) in a  $\beta$ -cell, suggesting that the cell was a glucose-sensitive  $\beta$ -cell. The bars indicate the puff time of 20 mM glucose from the puffing pipette ( $n = 20$ ).



The inactivation rate at the physiological resting membrane potential ( $-70$  mV) was surprisingly fast in  $\beta$ -cells, but not in ACCs. Figure 4A shows the ramp-potential-induced  $\text{Na}^+$  currents. To remove the inactivation of  $\text{Na}^+$  channels,

the holding potential was  $-120$  mV for both  $\beta$ -cells and ACCs before stimulation. The  $\text{Na}^+$  current was strongly dependent on the slope of the voltage ramp in  $\beta$ -cells; the fast-inactivating  $\text{Na}^+$  current was only visible during the

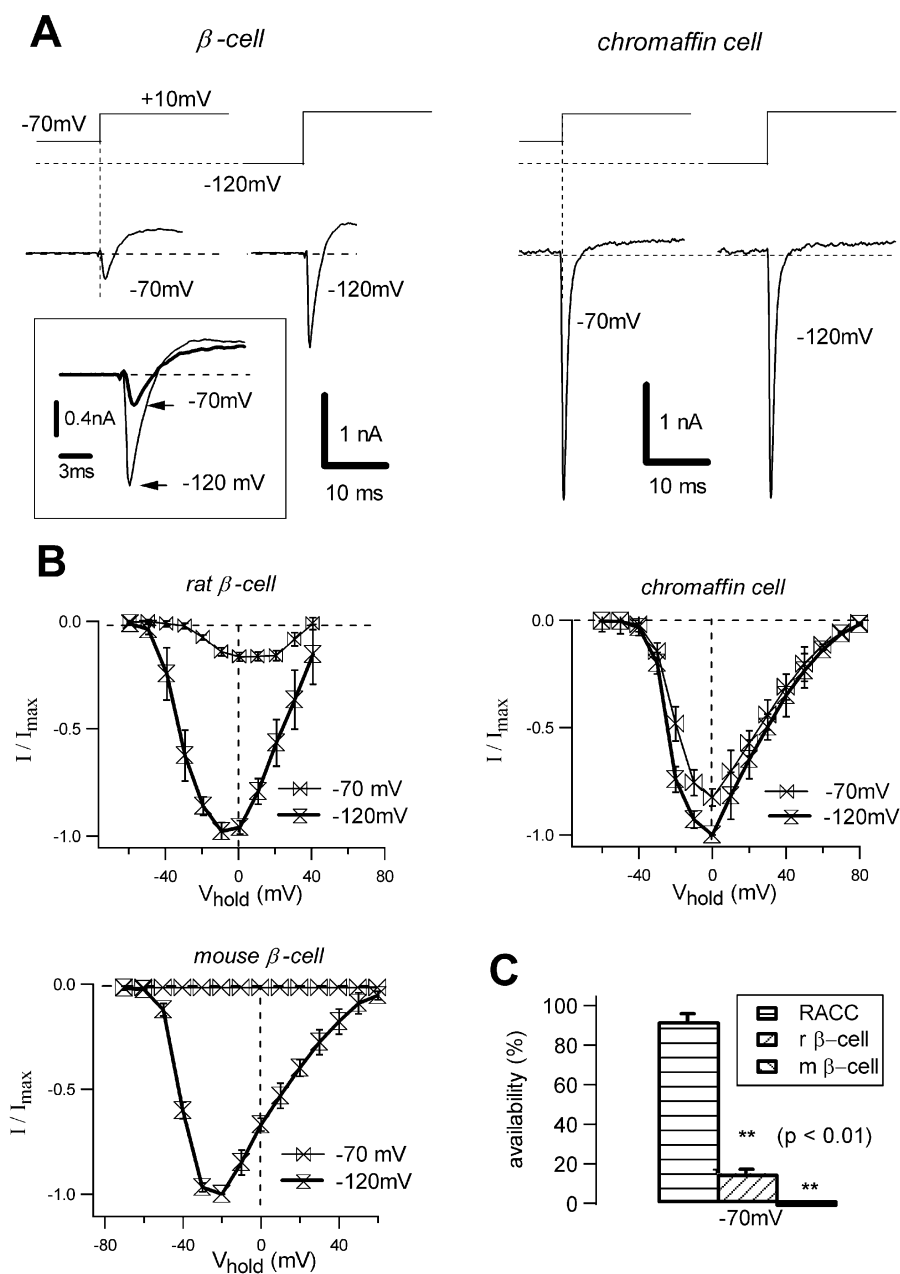


**Figure 2. Hyperpolarization is necessary for depolarization-induced  $\text{Na}^+$  currents in  $\beta$ -cells, but not in adrenal chromaffin cells (ACCs)**

A, fast inward  $\text{Na}^+$  currents induced by voltage pulses from either  $-70$  mV or  $-120$  mV to  $+10$  mV for 100 ms in a  $\beta$ -cell (left panel) and in an ACC (right panel). Depolarization from holding potential ( $V_{\text{hold}}$ )  $-120$  mV induced large  $\text{Na}^+$  currents in both types of cells. However, when  $V_{\text{hold}}$  was  $-70$  mV, the depolarization-induced  $\text{Na}^+$  current declined by 70% (average  $89 \pm 6\%$ , see panel C) in the rat  $\beta$ -cell (left panel). In the ACC (right panel), the depolarization-induced  $\text{Na}^+$  current was intact even at  $V_{\text{hold}} = -70$  mV. B, statistics of current-voltage curves of  $\text{Na}^+$  currents in rat ( $n = 12$ ) and mouse ( $n = 4$ )  $\beta$ -cells and in ACCs ( $n = 7$ ). C, statistics of hyperpolarization effect on  $\text{Na}^+$  currents. Availability is the percentage of  $\text{Na}^+$  current available at  $-70$  mV in contrast to that at  $-120$  mV. At  $V_{\text{hold}} = -70$  mV, the  $\text{Na}^+$  current was  $14 \pm 9\%$  of that at  $V_{\text{hold}} = -120$  mV in rat  $\beta$ -cells (r  $\beta$ -cell,  $n = 12$ ). In mouse  $\beta$ -cells (m  $\beta$  cell), the  $\text{Na}^+$  current was completely inactivated ( $n = 4$ ). The  $\text{Na}^+$  current was  $92 \pm 4\%$  of that at  $V_{\text{hold}} = -120$  mV in rat ACCs (RACC,  $n = 7$ ).

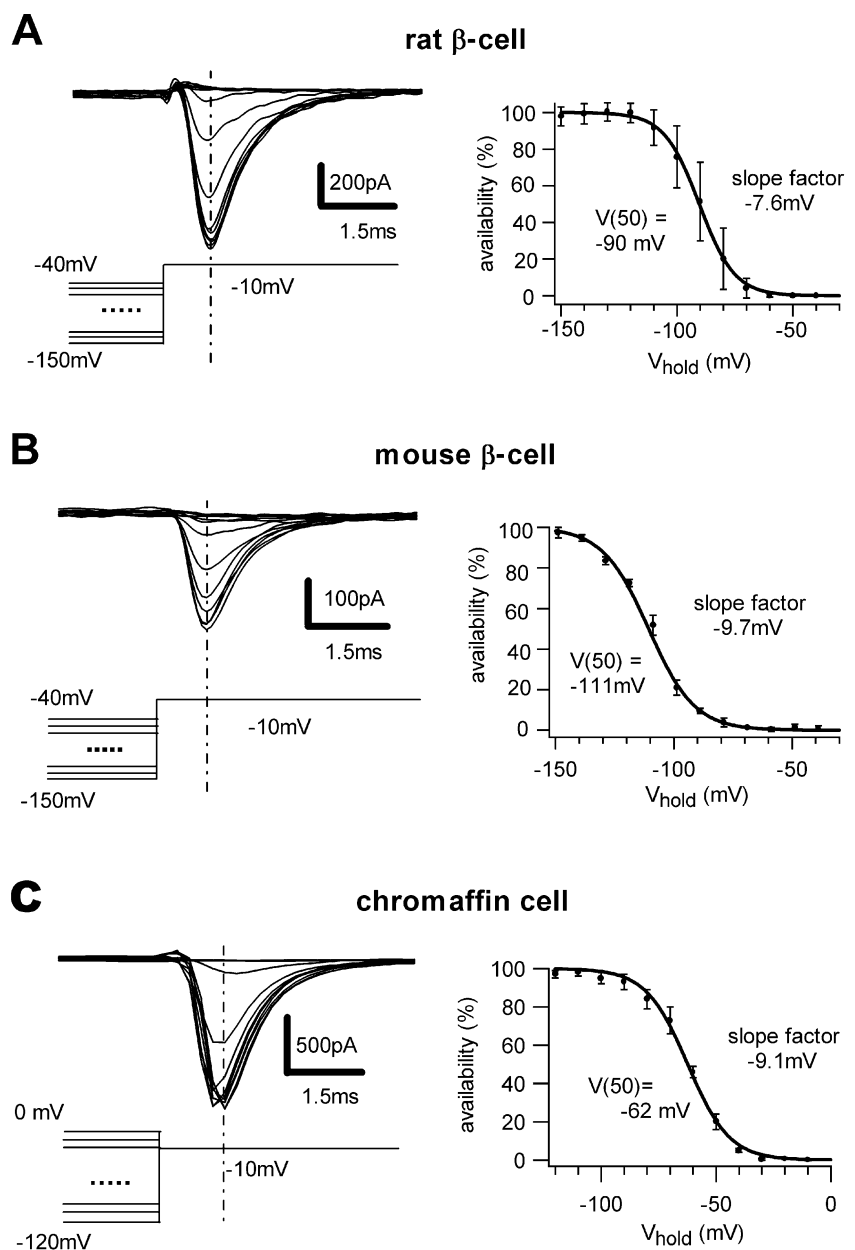
10 ms ramp. When the ramp duration was 30 ms or longer, all Na<sup>+</sup> currents disappeared. In contrast, the Na<sup>+</sup> current was similar to or even increased slightly for all ramp durations from 10 to 90 ms in ACCs. The protocol of five ramp potentials from -150 mV to +60 mV with ramp durations of 10, 30, 50, 70 and 90 ms, was the same for  $\beta$ -cells (Fig. 4A, left panel) and ACCs (Fig. 4A, right panel). To study the mechanism of the voltage slope dependence, we examined the time dependence of inactivation at a given 'prepulse potential'. As illustrated in Fig. 4B, the holding potential was -150 mV for both cell types. In each recording, a dual-pulse protocol was applied; the prepulse from -150 mV to -70 mV was followed by a second pulse from -70 mV to 0 mV. Note the peak Na<sup>+</sup> current was gradually reduced when the prepulse duration increased from 0 to 40 ms in  $\beta$ -cells (Fig. 4B, left panel). In contrast, increased prepulse duration had little effect on the Na<sup>+</sup> currents in ACCs (Fig. 4B, right panel).

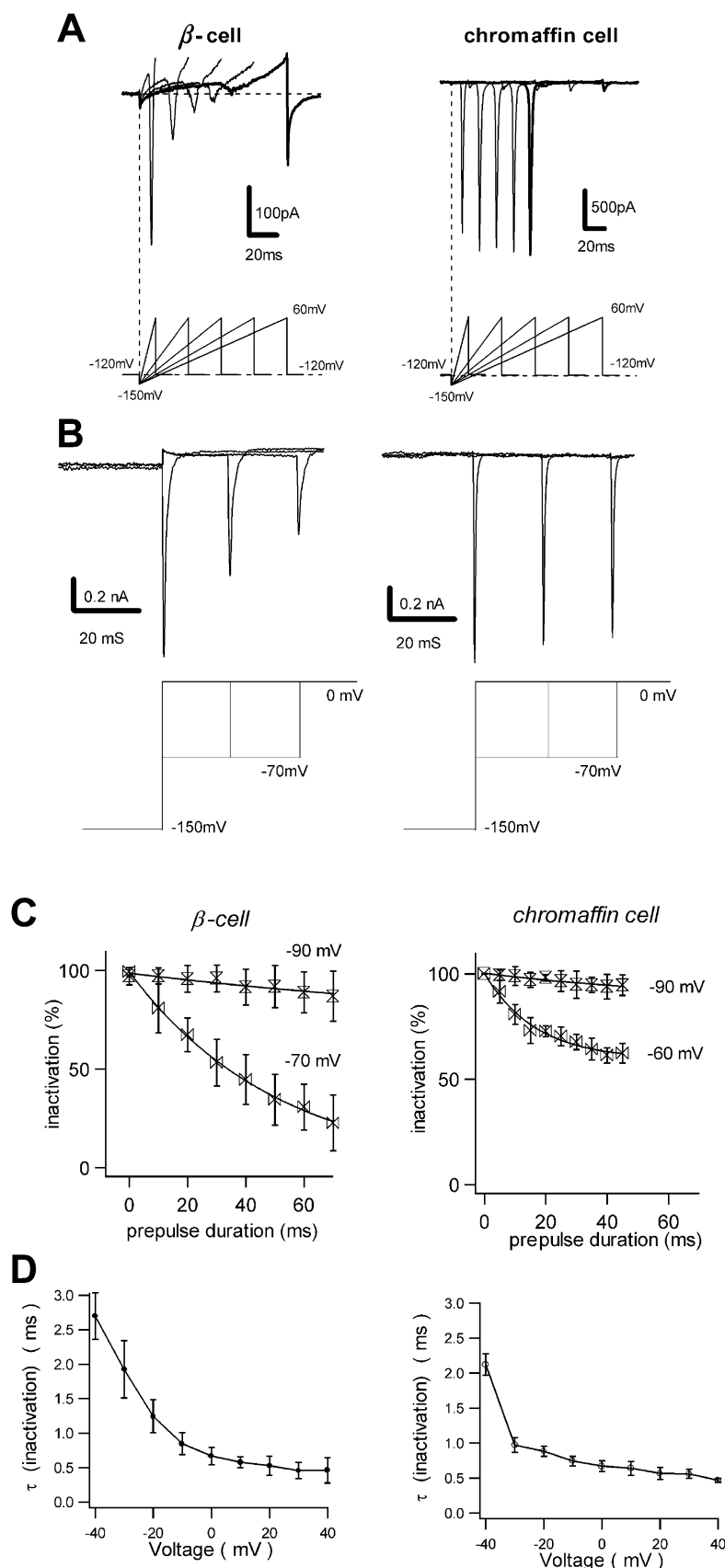
For rat  $\beta$ -cells, the experiments shown in Fig. 4B suggested that 65% inactivation of Na<sup>+</sup> channels took only 20 ms when the membrane potential increased from -150 mV to -70 mV. This explained why the Na<sup>+</sup> currents disappeared in the experiment illustrated in Fig. 4A when the voltage slope was 67 V s<sup>-1</sup> or slower.

Figure 4C shows the dependence of the inactivation on the prepulse voltage. The data were well fitted with single exponent functions for a given potential. In rat  $\beta$ -cells, the time constant of inactivation was 51 ms and 166 ms at -70 mV and -90 mV, respectively. After a 50 ms prepulse, the inactivation value was 65% and 10% for prepulse voltages of -70 mV and -90 mV, respectively. Note that the time constants can be inaccurate when they are longer than the protocol used to measure them. In ACCs, the time constant of inactivation was 17 ms and 69 ms at -60 mV and -90 mV, respectively. After a 50 ms prepulse, the

### Figure 3. Steady-state inactivation/availability of Na<sup>+</sup> currents.

The prepulse duration was 500 ms, which was sufficient to reach the steady-state of Na<sup>+</sup> channels in both cell types. **A**, steady-state inactivation of the Na<sup>+</sup> current in rat  $\beta$ -cells. The currents were induced by a dual-pulse protocol as included in the figure. The  $V_{\text{hold}}$  for 50% inactivation of the Na<sup>+</sup> current ( $V_{50}$ ) was -90 mV, and the slope factor was -7.6 mV ( $n = 12$ ). The data were fitted with the Boltzmann function (see Methods). **B**, steady-state inactivation of the Na<sup>+</sup> current in mouse  $\beta$ -cells.  $V_{50}$  was -110 mV and the slope factor was -9.7 mV ( $n = 4$ ). **C**, steady-state inactivation of the Na<sup>+</sup> current in ACCs.  $V_{50}$  was -62 mV, and the slope factor was -9.1 mV ( $n = 7$ ).





**Figure 4. Kinetics of inactivation differs in  $\beta$ -cells and ACCs**

A, slow ramp potential inhibited the  $\text{Na}^+$  current in a  $\beta$ -cell (left panel) but not in an ACC (right panel). In the lower traces, the different ramps are superimposed, and correspond to the whole-cell currents in the top traces. Note that the typical ramp-induced  $\text{Na}^+$  current (fast inward current) was dramatically reduced for slower ramp slopes in  $\beta$ -cells ( $n = 7$ ), but not in ACCs ( $n = 7$ ). B, the duration of the prepulse at  $-70$  mV determined the  $\text{Na}^+$  current in  $\beta$ -cells, but not in ACCs. In  $\beta$ -cells, 35% of the  $\text{Na}^+$  current inactivated during a 20 ms prepulse of  $-70$  mV ( $n = 11$ ). There was little inactivation of  $\text{Na}^+$  channels in ACCs ( $n = 7$ ). C, prepulse-duration-induced inactivation (from the closed state) was a function of the prepulse voltage. Using the protocol shown in B, in  $\beta$ -cells, the time constant of inactivation of the  $\text{Na}^+$  current was 51 ms and 166 ms at a prepulse potential of  $-70$  mV and  $-90$  mV, respectively (left panel,  $n = 6$ ). In ACCs, these time constants were 17 ms and 69 ms at  $-60$  mV and  $-90$  mV, respectively (right panel,  $n = 7$ ). Each trace was fitted by single exponential function. See text for voltage dependence of inactivation levels. D, the time constants of  $\text{Na}^+$  current inactivation (from the open state) were voltage dependent. The vertical axis shows time constants of  $\text{Na}^+$  channel inactivation induced by a step pulse from  $-120$  mV in rat  $\beta$ -cells (left panel,  $n = 12$ ) and ACCs (right panel,  $n = 7$ ).

inactivation value was 37% and 6% for prepulse voltages of -60 mV and -90 mV, respectively. Thus, the inactivation process of 'silent Na<sup>+</sup> channels' was three times slower in rat  $\beta$ -cells than in ACCs. However, at resting potential, a much larger fraction of Na<sup>+</sup> channels was inactivated in rat  $\beta$ -cells than in ACCs.

For non-silent Na<sup>+</sup> channels, the kinetics were quite similar in both of the cell types. Figure 4D shows the voltage dependence of inactivation of pulse-activated Na<sup>+</sup> currents. The protocol used was similar to that used to obtain the standard current-voltage curve shown in Fig. 2, except that the holding potential was fixed at -120 mV. For both cell types, the inactivation time constant was about 1 ms, corresponding to depolarization of -10 mV. The time constant increased by about twofold when the depolarization was -30 mV in both cell types.

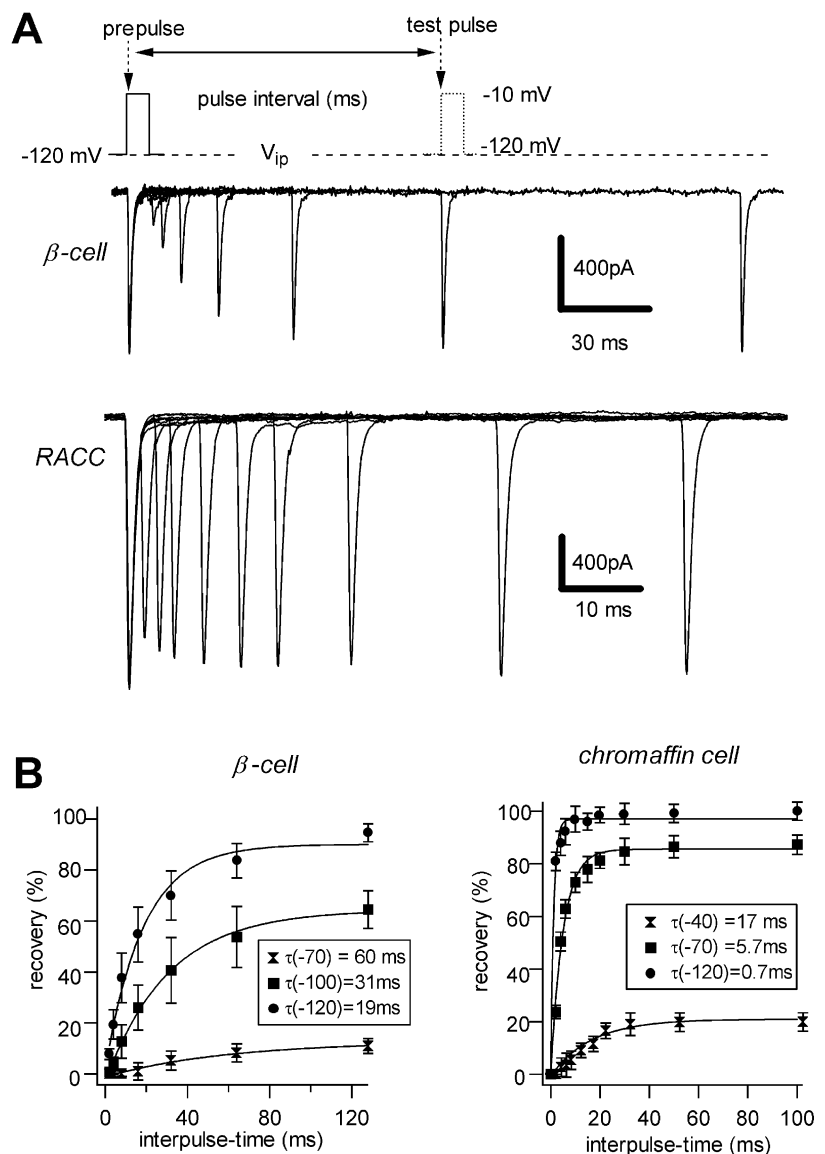
**Recovery from inactivation**

The Na<sup>+</sup> channels recovered from inactivation when the membrane potential was hyperpolarized. The time required

for the recovery could be tested by a dual-pulse protocol, as illustrated in Fig. 5A. The dual pulse included two 10 ms pulses; the first prepulse was from a holding potential of -120 mV to -10 mV and finished at a given interpulse potential ( $V_{ip}$ ), then the second (test) pulse was from  $V_{ip}$  to -10 mV and finished at the holding potential. The recovery was defined as the percentage of the Na<sup>+</sup> current induced by the second pulse versus that induced by the first pulse. The interval between the pre- and test-pulses was varied. The cells were held at given holding potentials for > 5 s between dual-pulse stimulations, so that the Na<sup>+</sup> channels reached steady state before the next dual-pulse stimulation. As shown in Fig. 5A, while the Na<sup>+</sup> current induced by the first pulse was the same for all dual-pulse stimulations, the Na<sup>+</sup> current induced by the second pulse was strongly dependent on the interpulse time in both rat  $\beta$ -cells and ACCs. Surprisingly, the recovery was much slower in  $\beta$ -cells than in ACCs. The recovery from inactivation was a function of both the pulse interval and  $V_{ip}$  in both cell types (Fig. 5B). The recovery curves were

**Figure 5. Time course of Na<sup>+</sup> channel recovery:  $\beta$ -cells are slower than ACCs**

A, time course of recovery of the Na<sup>+</sup> current from inactivation. The dual-pulse protocol is shown in the top trace. By changing the pulse interval time, a series of dual pulse-induced currents were superimposed according to pulse time. The interpulse potential ( $V_{ip}$ ) was -120 mV for both cell types. Note difference in time scale for the  $\beta$ -cells ( $n = 5$ ) and ACCs ( $n = 12$ ). B, voltage dependence of the recovery time course. The recovery time constants were defined as in A with different values of  $V_{ip}$ , which were applied during each dual-pulse stimulation. Between two dual-pulse stimulations, the cell was held at -120 mV for at least 5 s. Each trace can be well fitted by a single exponential function with a time constant ( $\tau$ ) as given in the figure. For example,  $\tau(-70)$  was the time constant at  $V_{ip} = -70$  mV.



well fitted by single exponentials. Both the steady-state value and the time constant of the exponential fit were dependent on  $V_{ip}$ . The recovery was faster at more hyperpolarized potentials for both cell types. At  $-70$  mV, the recovery was about 10 times slower in rat  $\beta$ -cells than in ACCs. In  $\beta$ -cells, the recovery time constant at a  $V_{ip}$  of  $-70$ ,  $-100$  and  $-120$  mV was 60, 31 and 19 ms, respectively ( $n = 12$ ). In ACCs, the recovery time constant was 17, 5.7 and 0.7 ms when  $V_{ip}$  was  $-40$ ,  $-70$  and  $-120$  mV, respectively ( $n = 16$ ).

### Role of the $\text{Na}^+$ current in rat $\beta$ -cells

At resting potential, 89% of the  $\text{Na}^+$  channels were inactivated in Wistar rat  $\beta$ -cells. It was of interest to determine whether the  $\text{Na}^+$  channels, inactivated at physiological resting potentials, could contribute to generating action potentials from hyperpolarized potentials. Figure 6 illustrates the action potentials induced by injecting currents under current-clamp conditions. In the  $\beta$ -cells, the current-induced action potentials had a peak voltage of 49 and 19 mV from a resting potential of  $-120$  and  $-70$  mV, respectively. In ACCs, the induced action potentials had the same peak voltage (55 mV) when the holding potential was  $-120$  and  $-70$  mV. In addition,

there was a slight delay (2 ms) in action-potential firing from hyperpolarization *versus* normal resting potential, probably due to the time needed for the voltage to increase from hyperpolarization to the normal resting level. The depolarization-induced action potentials were not affected by the hyperpolarization after the action potential was initiated. Thus, the hyperpolarization was critical in generating high-amplitude action potentials in rat  $\beta$ -cells, but not in ACCs. Note that the amplitude of action potentials in intact  $\beta$ -cells could be smaller because they were dependent on injection currents (data not shown, see Magistretti *et al.* 1998, for possible artefact in action-potential amplitude caused by the patch-clamp amplifier).

Further evidence for a possible role of  $\text{Na}^+$  channels in rat  $\beta$ -cells was provided by the observation that under whole-cell voltage-clamp conditions, the depolarization-induced  $\text{Na}^+$  currents were reversibly blocked by  $1 \mu\text{M}$  TTX (Fig. 7A). Figure 7B shows another cell under on-cell recording conditions with the pipette potential at 0 mV. Typical single K(ATP)-channel currents were activated before applying tolbutamide, which blocked the K(ATP) current completely. The blockade of K(ATP) currents induced the typical biphasic action currents, which were

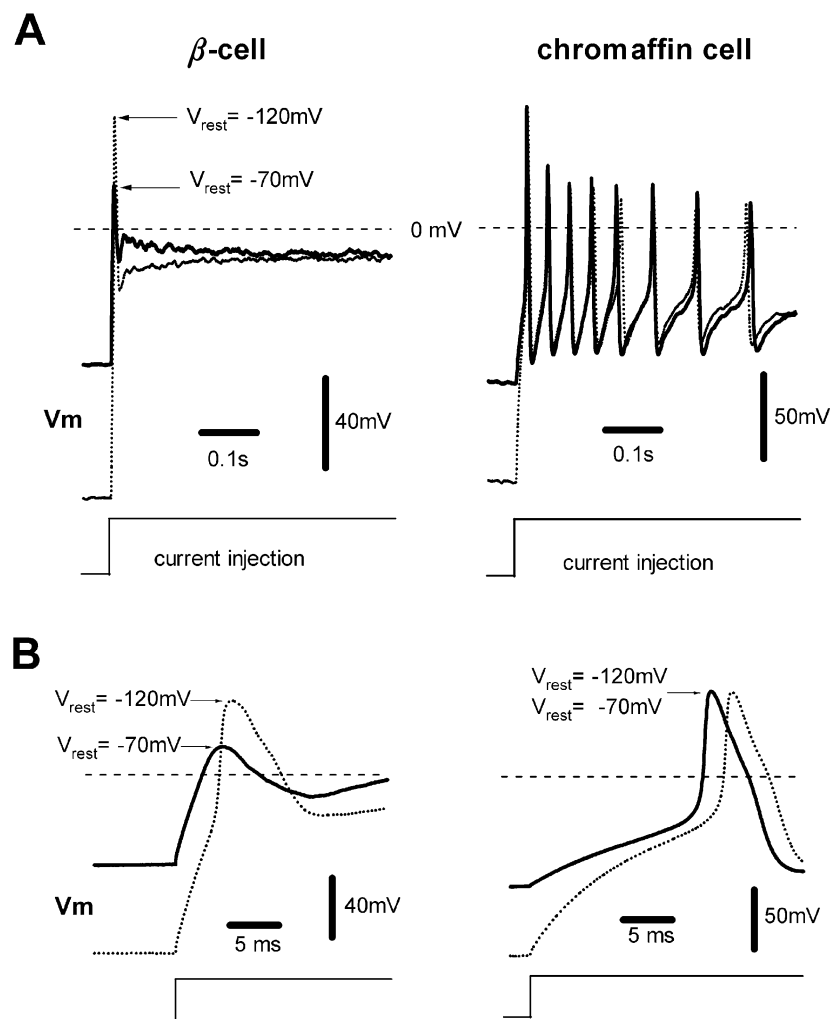


**Figure 6. Impact of hyperpolarization-sensitive  $\text{Na}^+$  channels on action potentials**

A, action potentials induced by injecting step currents. In  $\beta$ -cells, a 200 pA injection current induced a much larger amplitude of action potential when the resting potential ( $V_{rest}$ ) was  $-120$  mV than at  $-70$  mV, indicating that at  $-70$  mV the silent  $\text{Na}^+$  channels could increase action potential amplitude after recovery from inactivation ( $n = 20$ ). In ACCs, there was no difference in current-pulse-induced action potentials when  $V_{rest}$  was either  $-70$  mV or  $-120$  mV ( $n = 7$ ). B, the pulse-induced action potentials from A on an expanded time scale.  $V_m$  = membrane potential.



interpreted as action potential signals recorded in the on-cell patch-clamp configuration (Fenwick *et al.* 1982a; Misler *et al.* 1986; Plant, 1988). These action currents were blocked by TTX, indicating that Na<sup>+</sup> channels are involved in generating the action currents/potentials in Wistar rat  $\beta$ -cells. This conclusion is consistent with the report by Hiriart & Matteson (1988) that TTX can inhibit insulin secretion in Sprague-Dawley (SD) rat  $\beta$ -cells.

In some cells, Na<sup>+</sup> influx could affect secretion by affecting Na<sup>+</sup>-Ca<sup>2+</sup> exchange, which regulates the microdomain of Ca<sup>2+</sup> concentrations (Leblanc & Hume, 1990). The large number of 'silent Na<sup>+</sup> channels' in  $\beta$ -cells could increase Na<sup>+</sup> influx dramatically if the cells could recruit them under certain conditions. To test the role of Na<sup>+</sup> ions in secretion, we performed  $C_m$  measurements, which showed that an increase in  $C_m$  ( $\Delta C_m$ ) was induced by trains of depolarizing pulses (Fig. 8).  $\Delta C_m$  is a measure of the total number of secreted vesicles (Lindau & Neher, 1988; Zhang & Zhou, 2002). Na<sup>+</sup> currents were reduced by 70% when the holding potential was changed from -120 mV (Fig. 8,

left and right panels) to -70 mV (Fig. 8, middle panel). However,  $\Delta C_m$  signals were nearly identical for holding potentials of -120 mV and -70 mV, suggesting that Na<sup>+</sup> influx through Na<sup>+</sup> channels has little effect on insulin secretion in rat  $\beta$ -cells.

## DISCUSSION

In the present work, we found that the distinct inactivation behaviour of  $\beta$ -cells is one of the factors responsible for the dramatic differences in action potentials between  $\beta$ -cells and ACCs. These include: (1) the voltage-dependent steady-state inactivation, (2) the voltage-dependent recovery rate and (3) the kinetics of Na<sup>+</sup> channel inactivation at resting potential.

### Hyperpolarization sensitivity in $\beta$ -cells and ACCs

We found that up to 89% of Na<sup>+</sup> channels were silent at resting potential in rat  $\beta$ -cells (Fig. 2). In contrast, > 70% of Na<sup>+</sup> channels could be activated at resting potential in ACCs (Fig. 2). The silent Na<sup>+</sup> channels in  $\beta$ -cells could

**Figure 7. TTX-sensitive 'action currents' in rat  $\beta$ -cells**

A, TTX-sensitive Na<sup>+</sup> current under voltage-clamp conditions. TTX (1  $\mu$ M) blocked the Na<sup>+</sup> current nearly completely and reversibly. The inset shows the time course of TTX blockade ( $n = 5$ ). B, single-channel recording of K(ATP) and tolbutamide-sensitive action currents in the cell-attached patch-clamp configuration. The patch pipette was held at 0 mV and membrane current was filtered by a low-pass filter at 500 Hz. Single-channel currents of K(ATP) were blocked by 200  $\mu$ M tolbutamide. After blockade of K(ATP), biphasic action currents appeared, which were interpreted as being the result of action potentials in the cells. These action currents were blocked by adding 1  $\mu$ M TTX to the puff solution. K(ATP) currents recovered after removing tolbutamide.

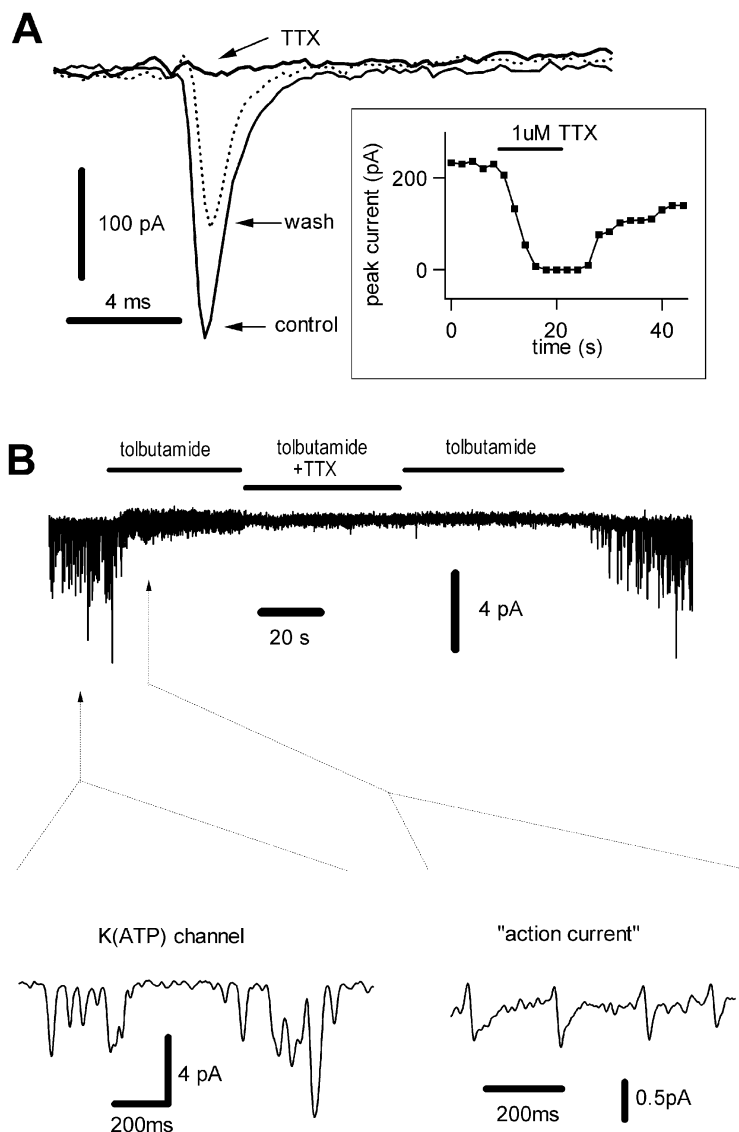


**Table 1. Inactivation of Na<sup>+</sup> channels in different species of pancreatic  $\beta$ -cells**

	Chromaffin	$\beta$ -cell (dog)	$\beta$ -cell* (human)	$\beta$ -cell (Sprague-Dawley rat)	$\beta$ -cell (Wistar rat)	$\beta$ -cell (mouse)
$E_{50}$ (mV)	-60	-60	-50	-80	-90	-110
$V_{10-90}$ (mV)	32	30	30	45	65	50
References	This work	Pressel & Misler, 1990	Barnett <i>et al.</i> 1995	Hiriart & Matteson, 1988	This work	This work

$E_{50}$  is the holding potential at which 50 % of Na<sup>+</sup> currents were inactivated, and  $V_{10-90}$  is the voltage of holding potential range in which Na<sup>+</sup> channels were inactivated from 10 % to 90 %. \* There are three types of human  $\beta$ -cells, those with Na<sup>+</sup> channels that are dog-like, intermediate and rat-like. These values were from dog-like cells (Misler *et al.* 1992; Barnett *et al.* 1995).

only be restored if a hyperpolarization voltage was applied (Fig. 4). The  $V_{50}$  was about -90 mV in rat  $\beta$ -cells. In mouse  $\beta$ -cells,  $V_{50}$  was -110 mV, which is consistent with previous reports (-109 mV, Plant, 1988; or -104 mV, Gopel *et al.* 1999). These differences in Na<sup>+</sup>-channel inactivation between  $\beta$ -cell and chromaffin cell are significant because Na<sup>+</sup> channels are primarily responsible for the rising phase and the short duration of an action potential. When a cell fires from its resting potential after a small depolarization, the upstroke amplitude is determined by the number of Na<sup>+</sup> channels available. Because at resting potential 70–90 % of the Na<sup>+</sup> channels are inactivated, the availability of Na<sup>+</sup> channels for activation in Wistar rat  $\beta$ -cells is lower than in ACCs. Thus, the action potential amplitude is much lower in  $\beta$ -cells (Fig. 6).

#### Fast inactivation at resting potential in rat $\beta$ -cells

Most Na<sup>+</sup> currents in the  $\beta$ -cells of other species are sensitive to TTX. In the present study, the Na<sup>+</sup> channels in Wistar rat

$\beta$ -cells were also sensitive to TTX, indicating that they are similar to standard Na<sup>+</sup> channels in this respect. This suggests that Na<sup>+</sup> channels in rat contribute to islet bursting, which is associated with plateau depolarization in 11.1 mM glucose (Ashcroft & Rorsman, 1989).

However, it was surprising that we could not see the fast inward Na<sup>+</sup> currents induced by a standard 100 ms ramp potential (-100 mV to +100 mV), even when the holding potential was -120 mV, whereas all Na<sup>+</sup> channels could be activated by a step depolarization. In contrast, the same ramp induced normal Na<sup>+</sup>-channel responses in ACCs. Further experiments demonstrated that the inhibition of ramp-induced Na<sup>+</sup> currents in  $\beta$ -cells depended on the ramp duration. Ramp-induced Na<sup>+</sup> currents appeared only when the ramp duration was shorter than 10 ms (Fig. 4A). Experiments using step pulses of variable duration revealed that the 'lost'  $\beta$ -cell Na<sup>+</sup> current during the ramp stimulus was because half of the Na<sup>+</sup> current

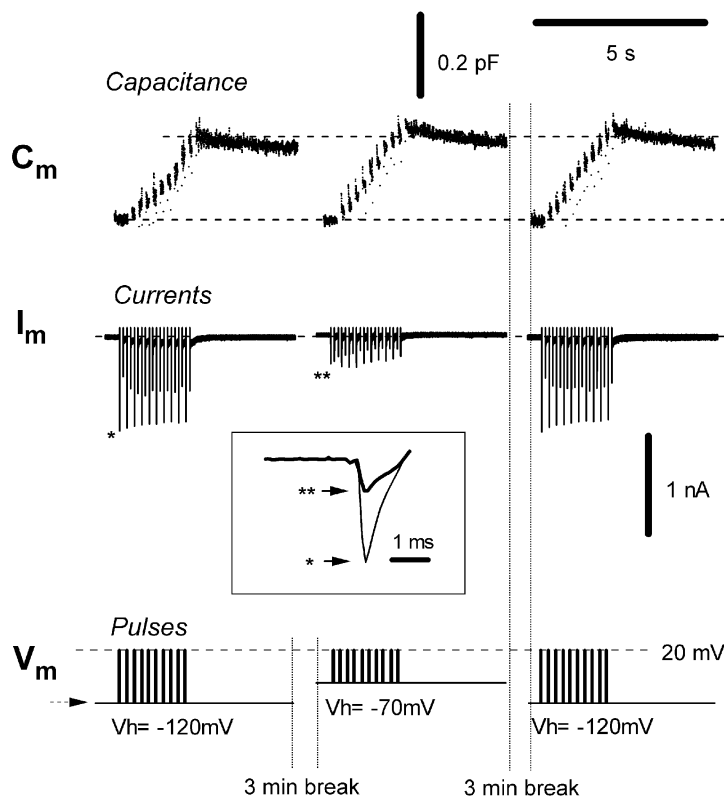


**Figure 8. Inactivation of Na<sup>+</sup> channels at -70 mV does not affect depolarization-induced secretion in  $\beta$ -cells**

The cell was stimulated by three identical trains of depolarizing pulses (10 × 100 ms pulses, with 100 ms interval between two pulses) from -120 mV (left and right panels) or -70 mV (middle panel) to 20 mV. To emphasize the Na<sup>+</sup> current in the middle panel, most outward K<sup>+</sup> currents were cut out and are not shown. The inset shows on an expanded time scale two examples of the Na<sup>+</sup> current marked by \* and \*\*. As shown in middle traces and the inset, most Na<sup>+</sup> currents were inhibited by holding the potential at -70 mV. However, depolarization-induced secretion (changes in membrane capacitance,  $C_m$ ) was nearly identical (200 pF) for both holding potentials of -70 mV and -120 mV, suggesting that Na<sup>+</sup> influx did not affect secretion. The basal  $C_m$  was 5.8 pF before stimulation. There were no significant changes in series conductance and membrane conductance before and after the stimulations ( $n = 8$ ). Bath temperature was maintained at 31–33 °C because  $\beta$ -cells do not secrete well at room temperature (Misler *et al.* 1992).  $I_m$  = membrane current.

inactivated within 40 ms at  $-70$  mV (Fig. 4B). This new finding in rat  $\beta$ -cells suggests that the short duration (51 ms) during which Na<sup>+</sup> channels inactivate from the closing state makes it difficult to recruit the silent Na<sup>+</sup> channels in  $\beta$ -cells for excitation. This means that even when the cell membrane is hyperpolarized, the silent Na<sup>+</sup> channels can contribute to action potentials only if the rise time from the hyperpolarization potential to  $-40$  mV (minimum potential to activate Na<sup>+</sup> channels) is less than 15 ms. We believe that this is one explanation for the lower amplitude (0–10 mV) of action potentials in rat  $\beta$ -cells. In ACCs, although the time constant to inactivate Na<sup>+</sup> channels from the closing state is even faster (17 ms) than in  $\beta$ -cells, the steady state extent of inactivation is much smaller (8% vs. 85%, see Fig. 2C).

### The physiological role of Na<sup>+</sup> channels in $\beta$ -cells

In contrast to  $\beta$ -cells, ACCs can recruit nearly 80% of the Na<sup>+</sup> channels at resting potential and fire tonic bursting action potentials with high amplitudes (30–60 mV, see Fig. 7). In dog  $\beta$ -cells, about 60% of Na<sup>+</sup> channels are not inactivated, and large action potentials can be generated from resting potential (Pressel & Misler, 1990). Human  $\beta$ -cells have both rat-type and dog-type action potentials (Rorsman *et al.* 1986; Barnett *et al.* 1995). Wistar and SD rat  $\beta$ -cells can recruit 11% and 50% of Na<sup>+</sup> channels at  $-70$  mV, respectively (this work; Hiriart & Matteson, 1988). The action potential in rat  $\beta$ -cells (Fig. 7, Zhou & Misler, 1996) is smaller than in human  $\beta$ -cells (Misler *et al.* 1992). It is possible that hyperpolarization is necessary to re-prime the rat Na<sup>+</sup> channels; for example, during a train of action potentials, large afterhyperpolarizations might allow more Na<sup>+</sup> channel availability than in a cell at its resting potential. In mouse  $\beta$ -cells, all Na<sup>+</sup> channels are inactivated at  $-70$  mV, and Na<sup>+</sup> channels have no effect on the Ca<sup>2+</sup>-dependent action potentials (Figs 2 and 3 of this work; Plant, 1988; Gopel *et al.* 1999). Taken together, it appears that in  $\beta$ -cells, the silent Na<sup>+</sup> channels of different species form an excitability series, with dog > human > SD rat > Wistar rat > mouse. We may define a score for fractional availability at a holding potential of  $-70$  mV for Na<sup>+</sup> channels (Table 1). Thus, mouse scores 0 because 0% of Na<sup>+</sup> channels are available at  $-70$  mV. Wistar and SD rats score 11 and 50, respectively (Fig. 3 of this work; Hiriart & Matteson, 1988). Human and dog score 40–60. ACCs score 70 because 70% of channels are available (Fig. 3). This explains why Na<sup>+</sup> channels have no physiological role in mouse  $\beta$ -cells (Plant, 1988; Ashcroft & Rorsman, 1990). In contrast,  $\beta$ -cells in dog, human and rat can contribute to cell excitability and secretion, although they do not contribute as much as Na<sup>+</sup> channels in neurons and ACCs (Figs 6 and 7 in this work and Hiriart & Matteson, 1988; Pressel & Misler, 1990; Barnett *et al.* 1995).

The density of Na<sup>+</sup> channels on the cell membrane is similar in the  $\beta$ -cells of different species. If we include the silent

channels, the Na<sup>+</sup> channel densities in  $\beta$ -cells (125 pA pF<sup>-1</sup>, assuming Na<sup>+</sup> current = 0.75 nA at  $-120$  mV,  $C_m$  = 8 pF) and ACCs (250 pA pF<sup>-1</sup>, assuming Na<sup>+</sup> current = 2.5 nA at  $-120$  mV,  $C_m$  = 10 pF) only differ twofold (Fig. 2 of this work; Hiriart & Matteson, 1988; Plant, 1988; Pressel & Misler, 1990; Barnett *et al.* 1995). Thus, differences in inactivation (especially steady-state inactivation) are critical. This could be explained by different  $\alpha$  subunits, different  $\beta$  subunits, or other modifications such as phosphorylation. Further work is needed to answer this open question.

## REFERENCES

- Aldrich RW (2001). Fifty years of inactivation. *Nature* **411**, 643–644.
- Armstrong CM & Bezanilla F (1977). Inactivation of the sodium channel. II. Gating current experiments. *J Gen Physiol* **70**, 567–590.
- Artalejo A (1995). Electrical properties of adrenal chromaffin cells. In *The Electrophysiology of Neuroendocrine Cells* ed. Hesheler J & Shcerubl H, pp. 259–300. CRC, Boca Raton, FL, USA.
- Artalejo CR, Rossie S, Perlman RL & Fox AP (1992). Voltage-dependent phosphorylation may recruit Ca<sup>2+</sup> current facilitation in chromaffin cells. *Nature* **358**, 63–66.
- Ashcroft FM, Harrison DE & Ashcroft SJ (1984). Glucose induces closure of single potassium channels in isolated rat pancreatic beta-cells. *Nature* **312**, 446–448.
- Ashcroft FM & Rorsman P (1989). Electrophysiology of the pancreatic beta-cell. *Prog Biophys Mol Biol* **54**, 87–143.
- Ashcroft FM & Rorsman P (1990). ATP-sensitive K<sup>+</sup> channels: a link between B-cell metabolism and insulin secretion. *Biochem Soc Trans* **18**, 109–111.
- Barnett DW, Pressel DM & Misler S (1995). Voltage-dependent Na<sup>+</sup> and Ca<sup>2+</sup> currents in human pancreatic islet beta-cells: evidence for roles in the generation of action potentials and insulin secretion. *Pflugers Arch* **431**, 272–282.
- Falke LC, Gillis KD, Pressel DM & Misler S (1989). ‘Perforated patch recording’ allows long-term monitoring of metabolite-induced electrical activity and voltage-dependent Ca<sup>2+</sup> currents in pancreatic islet B cells. *FEBS Lett* **251**, 167–172.
- Fenwick EM, Marty A & Neher E (1982a). A patch-clamp study of bovine chromaffin cells and of their sensitivity to acetylcholine. *J Physiol* **331**, 577–597.
- Fenwick EM, Marty A & Neher E (1982b). Sodium and calcium channels in bovine chromaffin cells. *J Physiol* **331**, 599–635.
- Gopel S, Kanno T, Barg S, Galvanovskis J & Rorsman P (1999). Voltage-gated and resting membrane currents recorded from B-cells in intact mouse pancreatic islets. *J Physiol* **521**, 717–728.
- Henquin JC, Bozem M, Schmeer W & Nenquin M (1987). Distinct mechanisms for two amplification systems of insulin release. *Biochem J* **246**, 393–399.
- Hille B (1992). *Ionic Channels in Excitable Cells*, 2nd edn. Sinauer, Sunderland, MA, USA.
- Hiriart M & Matteson DR (1988). Na<sup>+</sup> channels and two types of Ca channels in rat pancreatic B cells identified with the reverse hemolytic plaque assay. *J Gen Physiol* **91**, 617–639.
- Horn R & Marty A (1988). Muscarinic activation of ionic currents measured by a new whole-cell recording method. *J Gen Physiol* **92**, 145–159.
- Kidokoro Y & Ritchie AK (1980). Chromaffin cell action potentials and their possible role in adrenaline secretion from rat adrenal medulla. *J Physiol* **307**, 199–216.

- Leblanc N & Hume JR (1990). Sodium current-induced release of calcium from cardiac sarcoplasmic reticulum. *Science* **248**, 372–376.
- Lindau M & Neher E (1988). Patch-clamp techniques for time-resolved capacitance measurements in single cells. *Pflügers Arch* **411**, 137–146.
- Magistretti J, Mantegazza M, de Curtis M & Wanke E (1998). Modalities of distortion of physiological voltage signals by patch-clamp amplifiers: a modeling study. *Biophys J* **74**, 831–42.
- Misler S, Barnett DW, Gillis KD & Pressel DM (1992). Electrophysiology of stimulus-secretion coupling in human beta-cells. *Diabetes* **41**, 1221–1228.
- Misler S, Falke LC, Gillis K & McDaniel ML (1986). A metabolite-regulated potassium channel in rat pancreatic B cells. *Proc Natl Acad Sci U S A* **83**, 7119–7123.
- Neely A & Lingle CJ (1992). Two components of calcium-activated potassium current in rat adrenal chromaffin cells. *J Physiol* **453**, 97–131.
- Pace CS (1979). Activation of Na<sup>+</sup> channels in islet cells: metabolic and secretory effects. *Am J Physiol* **237**, E130–135.
- Plant TD (1988). Na<sup>+</sup> currents in cultured mouse pancreatic B-cells. *Pflügers Arch* **411**, 429–435.
- Pressel DM & Misler S (1990). Sodium channels contribute to action potential generation in canine and human pancreatic islet B cells. *J Membr Biol* **116**, 273–280.
- Pressel DM & Misler S (1991). Role of voltage-dependent ionic currents in coupling glucose stimulation to insulin secretion in canine pancreatic islet B-cells. *J Membr Biol* **124**, 239–253.
- Rorsman P & Trube G (1986). Calcium and delayed potassium currents in mouse pancreatic beta-cells under voltage-clamp conditions. *J Physiol* **374**, 531–550.
- Rorsman P, Arkhammar P & Berggren PO (1986). Voltage-activated Na<sup>+</sup> currents and their suppression by phorbol ester in clonal insulin-producing RINm5F cells. *Am J Physiol* **251**, C912–919.
- Satin LS, Tavalin SJ & Smolen PD (1994). Inactivation of HIT cell Ca<sup>2+</sup> current by a simulated burst of Ca<sup>2+</sup> action potentials. *Biophys J* **66**, 141–148.
- Wu JJ, He LL, Zhou Z & Chi CW (2002). Gene expression, mutation, and structure-function relationship of scorpion toxin BmP05 active on SK(Ca) channels. *Biochemistry* **41**, 2844–2849.
- Zeng XH, Lou XL, Qu AL & Zhou Z (1999). Ca<sup>2+</sup> signals induced from calcium stores in pancreatic islet beta cells. *Chin Sci Bull* **44**, 2058–2062.
- Zhang C & Zhou Z (2002). Ca<sup>2+</sup>-independent but voltage-dependent secretion in mammalian dorsal root ganglion neurons. *Nat Neurosci* **5**, 425–430.
- Zhou M, Morais-Cabral JH, Mann S & MacKinnon R (2001). Potassium channel receptor site for the inactivation gate and quaternary amine inhibitors. *Nature* **411**, 657–661.
- Zhou Z & Misler S (1995). Action potential-induced quantal secretion of catecholamines from rat adrenal chromaffin cells. *J Biol Chem* **270**, 3498–3505.
- Zhou Z & Misler S (1996). Amperometric detection of quantal secretion from patch-clamped rat pancreatic beta-cells. *J Biol Chem* **271**, 270–277.
- Zhou Z & Neher E (1993). Mobile and immobile calcium buffers in bovine adrenal chromaffin cells. *J Physiol* **469**, 245–273.

#### Acknowledgements

We thank Dr Iain Bruce for reading the manuscript, and Dr Peter Rorsman and Mr Chen Zhang for technical advice in preparation of mouse  $\beta$ -cells. This work was supported by grants from Major State Basic Research Program of China (G2000077800), National Natural Science Foundation of China (39525009, 39970238, and 39970371), CAS and The Li Foundation Heritage Prize (San Francisco).